Characterization and evaluation of a tray dryer with change of position: kinetics and thermodynamic properties of the process, preserving the nutraceutical quality in Golden Delicious apple slices

Bernabé Laureano[1*]; Carlos Alberto Daza[2]; Alberto Mauricio Santos[3]; María de la Luz Riviello[4]; Rosalía Daza[5]

[1] Departamento de Ingeniería Agroindustrial, Universidad Autónoma Chapingo (UACh). Carr. Méx.-Tex., km 38.5, 56230, Chapingo, México.
[2] Universidad Anáhuac Veracruz, Campus Córdoba-Orizaba. Calle Universidad 100 Rancho San Emigdio, 94500 Córdoba, Veracruz, México.
[3] Ingeniería Agrícola y uso Integral del Agua (IAUIA). UACh. Chapingo, México.
[4] Colegio de Postgraduados, Campus Montecillo, Km. 36.5, Carr. Méx.-Tex., 56230, Montecillo, Texcoco, México.
[5] Tecnológico Nacional de México/Instituto Tecnológico Superior de Xalapa, Sección 5ª Reserva Territorial s/n, Col. Santa Bárbara 91096 Xalapa, Enríquez, Veracruz, México.
* Correspondence: bernabelaureano@gmail.com

Citation: Laureano, B., L., Daza, C.A., Santos, A.M., Riviello, M. de la L., Daza, R. (2024). Characterization and evaluation of a tray dryer with change of position: kinetics and thermodynamic properties of the process, preserving the nutraceutical quality in Golden Delicious apple slices. *Agro Productividad*. https://doi.org/10.32854/agrop.v17i10.2997

Academic Editor: Jorge Cadena Iñiguez
Associate Editor: Dra. Lucero del Mar Ruiz Posadas
Guest Editor: Daniel Alejandro Cadena Zamudio

Received: August 06, 2024.
Accepted: October 13, 2024.
Published on-line: November 11, 2024.

Agro Productividad, 17(10). October. 2024. pp: 155-176.

ABSTRACT

The drying kinetics in apple slices between 45-55 °C was studied until reach a moisture ratio of 10±2%. 8 thin layer drying models were statistically fitted where the Midilli-Kucuk model presented the best performance, moreover its drying constant increased with the temperature, effective diffusivity was ranged from 68.16 E^{-10}-2.28 E^{-08} m^2 s^{-1}, the Arrhenius factor and activation energy were 3.74 E^{-02} m^2 s^{-1} and 28.11 kJ mol^{-1}, the enthalpy decreased from 25.46-25.38 kJ mol^{-1}, the entropy was ranged between (−0.2728-−0.2730) kJ mol^{-1} K^{-1}, and the Gibbs free energy increased from 112.25-114.98 kJ mol^{-1}. The 45 °C treatment preserved the highest phenolic compounds (51.1±1.54 mg EAG 100 g^{-1}), while the initial activity of elimination of radicals was 766.9±91.4 and 973.3±103.4 μg mg^{-1} according to the DPPH and ABTS methods, the antioxidant activity shows an inverse behavior to the drying temperature. This work will allow to establish the temperature, time, moisture ratio and energy to drying apple slices according to local weather or under controlled conditions.

Keywords: Apple drying, mathematical modeling, effective diffusivity, phenolic compounds, antioxidant activity.

INTRODUCTION

The apple is a tree fruit cultivated in various parts of the world, its global production ranks third compared to other fruits, preceded by bananas and watermelons (Ghinea, Prisacaru, and Leahu, 2022). It is a natural food that possesses numerous nutritional properties, such as vitamins, minerals, and fiber (Noori *et al.*, 2021).

Like other fruits, apples provide nutrients and can prevent some diseases due to chemicals that modify the physiology of the organism.

These substances are compounds classified as secondary metabolites or phytochemicals, which contain bioactive properties. Additionally, this product has been characterized regarding its color and according to its antioxidant properties. Apples are consumed in various forms, whole, as dehydrated slices, as juice, in extract, pulverized, and in compote, as they possess diverse nutritional properties to prevent or control various diseases as obesity, cholesterol-related issues, and those related to the immune system.

In Mexico, apple crop yield fluctuates between 11-12 t ha^{-1}. By 2021, global production was estimated to exceed 93 000 000 tons with an average yield of 19-20 ton ha^{-1} (FAOSTAT, 2023). Apple dehydration is carried out either outdoors or in greenhouses with varying temperatures and times, meaning that these parameters are not controlled, relying solely on local environmental conditions, which results in reduced product quality. Dehydration technologies are useful for improving the quality of active ingredients and increasing post-harvest yields, reducing losses due to contamination or product deterioration, and minimizing energy consumption, as demonstrated by Martynenko and Janaszek (2014), who dehydrated and analyzed the texture of apple slices in a convective dehydrator at temperatures between 40-80 °C, or as stated by Solano and Rodríguez (2010), who agree that dehydrators are safe, efficient, and economically viable mechanisms in the post-harvest management of food products.

Several authors have studied the kinetics and mathematical modeling of thin-layer dehydration of food products, such as Inyang *et al.* (2018)for shelf life elongation, to minimize packaging and improving storage for easy transportation. Thin-layer drying of materials is necessary to understand the fundamental transport mechanism and a prerequisite to successfully simulate or scale up the whole process for optimization or control of the operating conditions. Researchers have shown that to rely solely on experimental drying practices without mathematical considerations for the drying kinetics, can significantly affect the efficiency of dryers, increase the cost of production, and reduce the quality of the dried product. An effective model is necessary for the process design, optimization, energy integration and control; hence, the use of mathematical models in finding the drying kinetics of agricultural products is very important. The statistical criteria in use for the evaluation of the best model(s who agree that dehydration modeling is highly useful for determining process behavior, maintaining product quality, and aiding in reducing product losses. Regarding the dehydration of fruits, the semi-empirical Midilli-K. model has shown the best fit, as demonstrated by Mugodo and Workneh (2021) in mango slices. Additionally, thermodynamic properties were determined, as conducted by Nadi and Tzempelikos (2018) in Golden Delicious slices.

Recent studies on apple slice dehydration exist, such as the one conducted by Royen *et al.* (2020)air humidity, air velocity and slice thickness on process kinetics, product water activity and parameters of empirical models has been investigated. Drying characteristics of apple slices were monitored at temperatures of 40, 45 and 50 °C, air velocities of 0.6, 0.85 and 1.1 m/s., slice thicknesses of 4, 6, 8, 10 and 12 mm, and in relative air humidity ranges of 25-28, 35-38 and 40-45%. During the process, samples were dried from an initial moisture content of 86.7% to that of 20% (w.b, based on five thin-layer models, using a convective tray dehydrator. Additionally, Noori *et al.* (2021) contrasted 11 models

within a temperature range of 33 to 55 °C. Both studies mentioned that the Midilli-K model represented dehydration best, although they did not delve into the study of its thermodynamic properties.

The aim of this work was to study the kinetics of thin-layer dehydration of Golden Delicious apple slices in a tray dryer with position change, through mathematical modeling and the fitting of dehydration curves. This aimed to evaluate, with a general expression, the effect of temperature on moisture content ratio, total phenolic content, and antioxidant activity.

MATERIAL AND METHODS

Dehydrator features

Dehydration is an operation involving heat and mass transfer. This process extends the shelf life of various food products by reducing the water activity to a sufficiently low level to inhibit microbial, enzymatic, and other deteriorating reactions (Sabarez, 2015).

The experimentation of the thin-layer dehydration process of Golden Delicious apple slices was carried out in a tray dryer with position change, constructed of stainless steel 304-L, with 6 trays measuring 0.27×0.74 m. Figure 1 illustrates the placement of sensors and actuators. This equipment is operated through a graphical interface created in Visual C Sharp software, allowing real-time monitoring of process variables (internal humidity, internal temperature, and airflow velocity at the dryer outlet).

The system consists of a 12 VDC. axial fan that generates air flow velocities of 3 m s^{-1}, located at the entrance of the equipment. Heat is generated by a 1600 W, 60 Hz electric resistance at 127 VA.C, controlled by a digital Autonics TCH-4 controller, with temperature ranges from 30-85 °C, measured by a type J thermocouple with a hysteresis of ±0.5 °C, as shown in Figure 2.

The tray position change during the dehydration process occurs every minute and lasts for 3 seconds, activated by an actuator coupled to the shaft (Figure 3a), which is a 20 Vc.d., 8 A geared motor with a variable rotation frequency between 0-280 rpm sufficient to provide freedom of movement (Figure 3b). This action is carried out in order to maintain heat homogeneity on the product surface and inside the dehydrator.

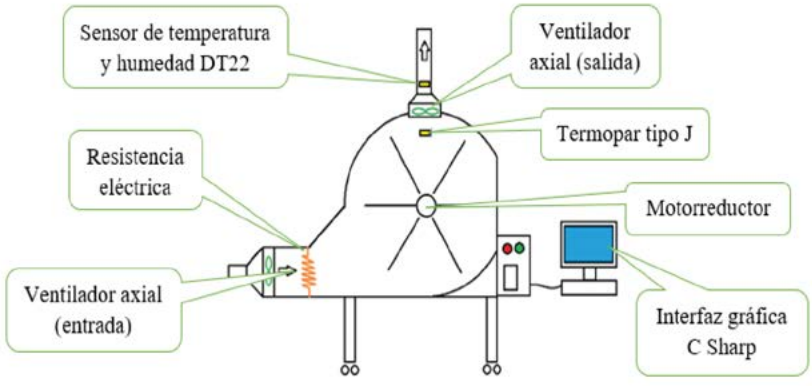

Figure 1. Scheme of the tray dehydrator.

Figure 2. Temperature controller and actuators.

Figure 3. Rotation system. (a) Coupled geared motor. (b) Tray distribution.

A 12 $V_{D.C.}$ axial fan, at the equipment's output, operates as an air extractor. When the percentage of moisture released by the product increases, the fan increases the airflow at the output.

In Figure 4, (a) the graphical interface, and (b) the communication with the physical system are observed, whose design allows the dehydrator to be autonomous under any external alteration or disturbance during its operation.

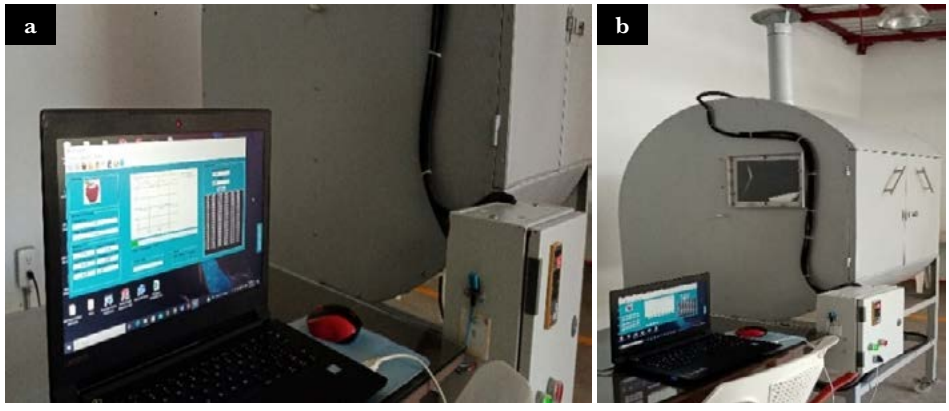

Figure 4. Rotary tray dryer. (a). Interface (b). Actuator connection.

Dehydration process

This research was conducted in Tehuacán, Puebla, located at 19° 29' N, 98° 53' W, at an altitude of 2240 meters. The experiment was based on a completely randomized design with a one-factor arrangement, considering temperature, T, as the sole factor, with 3 treatments ranging from (45-55) °C and $\Delta T=5$ °C, carried out in triplicate, resulting in 9 experimental units. The response variable was the moisture ratio, MR, as described in Equation 1.

$$MR=\frac{M_t-M_e}{M_o-M_e}\approx\frac{M_t}{M_o} \quad (1)$$

Where MR is the moisture ratio (dimensionless); M_t is the moisture ratio at time $t\left(g_{H_2O}\ g_{MS^{-1}}\right)$, M_o is the initial moisture ratio of the product $\left(g_{H_2O}\ g_{MS^{-1}}\right)$ and M_e is the equilibrium moisture ratio $\left(g_{H_2O}\ g_{MS^{-1}}\right)$.

The values of M_e were relatively small compared to M_t and M_o, and it should be noted that $M_e=0$ (Celma *et al.*, 2007).

The apples were purchased from a commercial center during the 2022 season and were conditioned for the dehydration process immediately. To minimize measurement errors, the samples were homogenized with respect to size, color, and ripeness level.

To measure the mass of the samples, m, an MA 50/1. R moisture analyzer (Radwag, Poly) was used (precision ±0.001 kg). Temperature was measured using a type J class 1 thermocouple with compacted mineral protection of two terminals and ceramic insulation with a range of −40 °C to +125 °C (precision ±1 °C). The airflow velocity, v, was measured using a TMA-10A anemometer (Amprobe, Netherlands) (precision ±0.01 m s^{-1}).

During the experiments, the temperature and airflow velocity remained constant at the inlet and outlet of the equipment, with some variations inside of ±3 °C and v=3 m s^{-1}. The initial mass of the product was $m=1$ kg per treatment. The fresh apple slices were placed inside the dryer, distributed among the 6 stainless steel trays, each measuring 0.1998 m^2. The diameter of the slices ranged from 0.065-0.075 m with a material thickness (L) of 0.0014 m. During the tests, the mass m was recorded every 3 minutes, ending when the product reached $MR=10\pm2\%$.

Drying rate. It is the change in MR per unit of time, Equation 2:

$$DR=\frac{MR_{t+\Delta t}-MR_t}{\Delta_t} \quad (2)$$

Where DR is the dehydration rate $\left(kg_{H_2O}\ kg_{MS^{-1}\ min^{-1}}\right)$ and Δt is the time period (min).

Dehydration kinetics

Mathematical Modeling

To predict the behavior of the process in apple slices, a statistical analysis of the data was conducted with respect to 8 thin-layer dehydration models (Table 1). The analysis and model fitting were performed using the Curve Fitting Tool included in Matlab v 9.3.

Using Equation 1, *MR* was determined to construct the *MR vs. t* curves. Additionally, the statistical selection criterion to calculate the goodness of fit of the 8 models to *MR* and determine which one best describes the dehydration process was: locating the highest value of the coefficient of determination, R^2, as well as the minimum values of the root mean square error, RMSE, and the sum of squares due to error, SSE (Inyang *et al.*, 2018).

Adjustment in the constant and coefficients of the model

The coefficients were estimated according to T, where *k* should be associated with the ease of removing moisture from the apple slices.

Generalization of the MR curve

The possibility of fitting the curve to the data by correlating *MR vs.* τ for the temperature range was verified (Menezes *et al.*, 2013), *i.e.*, to determine the behavior of the process at any time or moisture ratio within the study temperature range T. Equation 3:

$$\tau = \frac{N_c t}{MR_o} \tag{3}$$

Where τ is time (dimensionless), MR_o is the initial *MR* (dimensionless), and N_c is the dehydration rate constant (1 min^{-1}).

Table 1. Models evaluated for dehydrating apple slices.

Model	MR
Kaleta (Kaleta *et al.*, 2013)	$a \cdot e^{(-kt^n)} + (1-a) \cdot e^{(-bt^n)}$
Two term (Olawoye *et al.*, 2017)	$a \cdot e^{(-k_0 t)} + b \cdot e^{(-k_1 t)}$
Henderson and Pabis (Olawoye *et al.*, 2017)	$a \cdot e^{(-kt)}$
Logarithmic (Mghazli *et al.*, 2017)	$a \cdot e^{(-kt)} + c$
Midilli-K. (Ekka y Palanisamy, 2020)	$a \cdot e^{(-kt^n)} + b \cdot t$
Page (Tunckal *et al.*, 2018)	$e^{(-kt^n)}$
Diffusion Approximation (Şï mşek *et al.*, 2021)	$a \cdot e^{(-bt)} + (1-a) \cdot e^{(-bct)}$
Verma (Olawoye *et al.*, 2017)	$a \cdot e^{(-kt)} + (1-a) \cdot e^{(-gt)}$

Model Validation

The validation criterion was to plot adjusted *MR*, MR_{aj}, against experimental *MR*, MR_{ex}, for the applied T range (Benseddik *et al.*, 2018; Beye *et al.*, 2019).

Effective Diffusivity and Activation Energy

Effective Diffusivity

The mass transfer in the transient state of thin-layer dehydration of food products is studied using the expression of Fick's second law of diffusion. To establish the value of effective diffusivity, Deff, apple slices were considered as a body of planar geometry (Crank, 1979). Equation 4:

$$MR = \frac{8}{\pi^2}\sum_{i=0}^{\infty}\frac{1}{(2n+1)^2}e^{\left[-\frac{(2n+1)^2\pi^2 D_{eff}t}{4L^2}\right]} \tag{4}$$

Where D_{eff} is the effective diffusivity ($m^2\ s^{-1}$); L is the material thickness (m), and n is the number of terms (dimensionless).

Equation 4 assumes a uniform distribution of initial moisture content, simplifying diffusion movement and neglecting deformation. For extended dehydration periods, where $MR<0.6$ and $n=0$, Equation 5 is obtained (Tunçkal, 2020):

$$MR = \frac{8}{\pi^2}e^{\left[\frac{\pi^2 D_{eff}t}{4L^2}\right]} \tag{5}$$

Applying the law of logarithms to both sides of the previous equation yielded Equation 6, and by isolating ko, Equation 7, the value of D_{eff}: was determined:

$$\ln(MR) = \ln\left(\frac{8}{\pi^2}\right) - \left(\frac{\pi^2 D_{eff}t}{4L^2}\right) \tag{6}$$

$$k_o = \left(\frac{\pi^2 D_{eff}}{4L^2}\right) \tag{7}$$

where k_o (dimensionless) is the slope of the $\ln(MR)$ *vs. t* line (Mugodo y Workneh, 2021).

To estimate D_{eff}, Equation 5 was evaluated with the Fourier number, F_o (Mohammadi *et al.*, 2019), Equation 8:

$$F_o = \left(\frac{D_{eff}\, t}{L^2} \right) \tag{8}$$

where F_o is the Fourier number (dimensionless).

Rewriting Equation 5 and transforming it into its linear form resulted in Equations 9 and 10. By isolating Fo from Equation 10, Equation 11 was derived. Finally, in Equation 8, Deff was isolated and Fo was replaced with Equation 11.

$$MR = \frac{8}{\pi^2} e^{\left(\frac{\pi^2 F_o}{4} \right)} \tag{9}$$

$$\ln(MR) = -0.21 - 2.4674\ F_o \tag{10}$$

$$F_o = -0.4052 \ln(MR) - 0.0851 \tag{11}$$

Activation energy

Expresses the dependency of D_{eff} on temperature, representing the energy required to initiate the moisture diffusion reaction in the product (Ghasemkhani *et al.*, 2021). This dependency is evaluated using Equation 12.

$$D_{eff} = D_o e^{\left(-\frac{E_a}{RT} \right)} \tag{12}$$

where D_o is the frequency or pre-exponential factor of Arrhenius ($m^2\ s^{-1}$); *Ea* is the activation energy ($J\ mol^{-1}$); R is the universal gas constant ($8.3143\ J\ mol^{-1}\ K^{-1}$) and T is the absolute temperature (K). Linearizing Equation 12 yields:

$$\ln\left(D_{eff} \right) = \ln\left(D_o \right) - \frac{E_a}{RT} \tag{13}$$

The values of E_a are obtained by plotting $\ln(D_{eff})$ *vs.* $1\ T^{-1}$, where $E_a\ R^{-1}$ y $\ln(D_o)$ are the slope and intersection of the obtained line, confirming the correlation between D_{eff} and T, where E_a increases with lower L (Petković *et al.*, 2021). This should be considered when designing dehydration systems and calculating the energy required to remove the moisture content from the product.

Thermodynamic Properties

E Enthalpy, H, is the energy required to remove moisture from a product during dehydration and decreases with increasing temperature (Nadi and Tzempelikos, 2018).

Negative values indicate the absence of endergonic reactions, which require an external energy source for the product to transform.

Entropy, S, is the degree of disorder in the water-product system (Oliveira *et al.*, 2010). As temperature increases, the entropy of the system decreases (Costa *et al.*, 2016), increasing the diffusion rate of water from inside the product to the drying air (Araujo *et al.*, 2017).

Gibbs free energy, G, is the work done by the system during adsorption or desorption, and it also indicates the amount of water contained in the product, evaluating the loss of liquid from the material (Araujo *et al.*, 2017). Positive values of G indicate that there is no spontaneous variation in ΔG, meaning that dehydration is a non-spontaneous process, demonstrating that external energy contributions are required for this phenomenon to occur.

The above parameters were determined using the method of Jideani and Mpotokwana (2009), obtaining Equations (14-16):

$$\Delta H = E_a - RT \tag{14}$$

$$\Delta S = R\left[\ln\left(D_o\right) - \ln\left(\frac{k_B}{h_P}\right) - \ln(T)\right] \tag{15}$$

$$\Delta G = \Delta H - T\Delta S \tag{16}$$

where ΔH represents changes in H (J mol^{-1}), ΔS represents changes in S (J mol^{-1} K^{-1}), ΔG represents changes in G (J mol^{-1}), k_B is the Boltzmann constant ($1.38 \cdot E^{-23}$ J K^{-1}) and h_P is the Planck constant ($6.626 \cdot E^{-34}$ J s^{-1}).

Total Phenolic Compounds and Antioxidant Activity

Preparation of Extracts

A sample of 10 g of finely chopped fruit was homogenized with 20 mL of 80% (v v^{-1}) methanol and sonicated at 25±2 °C and 40 kHz for 20 min (Cole-Parmer, 08895, Vernon Hills, IL, USA) in the presence of inert gas (^{18}Ar) to prevent oxidative degradation of polyphenols. The extract was centrifuged at 5500×*g* for 20 min using a tabletop centrifuge (Eppendorf, 5804, Hamburg, Germany). The supernatant was collected for analysis of phenolic compounds and antioxidant capacity.

Total Phenolic Content

The total phenolic content (CFT) was determined using the colorimetric method of Folin-Ciocalteu (Corona-Leo *et al.*, 2021), which involves the oxidation of the phenolate ion along with the reduction of the phosphotungstic-phosphomolybdic reagent. The chromophore produced is a blue phosphotungstic-phosphomolybdic complex that has a maximum absorption in the region of 750 nm. For the determination, 1 mL of the prepared methanolic extract, 60 mL of distilled water, and 5 mL of Folin-Ciocalteu reagent were poured and mixed in a 100 mL volumetric flask. After 4 minutes, 15

mL of 7% (p v^{-1}) sodium carbonate was added, adjusting the volume to 100 mL using distilled water. The mixture was covered with aluminum foil and allowed to react for 30 minutes at room temperature (25±2 °C). Absorbance measurements were carried out at a wavelength of 750 nm using a single-beam UV-Visible spectrophotometer (LX510SS, Labdex, London, UK). The calibration curve was constructed using gallic acid as the standard with $n=6$ concentrations in the range of 0-500 mg L^{-1} and adjusted by linear regression ($R^2=0.995$). The results were expressed as mg gallic acid equivalents (EAG) per 100 g of sample (mg EAG 100 g^{-1} of dry weight of the sample).

Antioxidant Activity

The antioxidant activity exhibited by a metabolite is observed when it neutralizes any free radicals (Frei, 1994).

Free radical scavenging assays of DPPH and ABTS radical

Antioxidant activity was measured using the DPPH reagent method (2.2-diphenyl-1-picrylhydrazyl, Sigma-Aldrich; St. Louis, Missouri, USA) according to Bao *et al.* (2023). 1.2 mL of sample extract (Section 2.3.1) was mixed with 3.6 mL of methanol solution at a concentration of 5 mmol mL^{-1} DPPH. The mixture was kept in the dark at room temperature (25±2 °C) for one hour, and then the absorbance was measured at 517 nm. The DPPH scavenging velocity of the extract was calculated according to Equation 17 (Iordănescu *et al.*, 2021):

$$AER = \frac{A_0 - A_s}{A_s} 100 \quad (17)$$

where AER is the radical scavenging activity, A_0 is the absorbance of the blank or control sample, and A_s is the absorbance of the sample extract.

The ABTS assay (2.2'-azino-bis(3-ethylbenzothiazoline-6-sulfonic acid), Sigma-Aldrich; St. Louis, Missouri, USA) was conducted based on the methodology adapted from López-Vidaña *et al.*, (2019). The $ABTS^{+\cdot}$ radical cation was produced by reacting a mother solution of ABTS at a concentration of 7 mM with an oxidizing solution of potassium persulfate ($K_2S_2O_8$) at a concentration of 2.45 mM. The mixture was stored in the dark at room temperature (25±2 °C) for 24 hours prior to the experiments. Subsequently, the $ABTS^{+\cdot}$ solution was diluted with a 5 mM phosphate-buffered saline solution (pH 7.4) to obtain an absorbance of. 0.7±0.02 at $\lambda=730$ nm (t_0). Then, 0.1 mL of the sample extract was added to 3.9 mL of the diluted $ABTS^{+\cdot}$ solution. Additionally, absorbance readings were taken every 20 s using a spectrophotometer (LX510SS, Labdex, London, United Kingdom). The reduction of the radical was monitored for 6 minutes (t_6). The inhibition of absorbance vs time was plotted, and the area under the curve was calculated for the interval between 0 and 6 minutes. The degree of inhibition was calculated according to

Equation 18, and the antioxidant activity of the samples was expressed as μmoles ET 100 g^{-1} of dry weight of the sample.

$$\%_{inh} = \left(\frac{A_{t_0} - A_{t_6}}{A_{t_0}} \right) 100 \tag{18}$$

Where *inh* is the inhibition of absorbance (%), A_{t_0} , A_{t_6} are the absorbances during the time intervals t=0.6 min.

Statistical Analysis

For each sample, the results are presented as the mean ± standard deviation of three replicates. Differences between mean values were evaluated using Tukey's honestly significant difference (DHS) de Tukey, p≤0.05. Statistical calculations were performed using OriginPro 8.1 software (OriginLab; Northampton, MA, USA).

RESULTS AND DISCUSSION

Dehydration Process

Kinetics of Dehydration

According to Equation 1, MR_{ex} was obtained for different time intervals and dehydration temperature, T. Figure 5a shows $MR_{ex}-MR$ estimates, the MR_{est} curves, *vs. t* for different T values. As T increased, the values of t decreased from 2.9-2.1 h to achieve MR=10±2%, demonstrating that T was the parameter with the greatest influence on improving the duration of the process, similar to Beigi (2016), who reduced this parameter by 60% at 70 °C and 2 m s^{-1}. Figure 5b shows the fresh and processed apple slices according to Figure 5a.

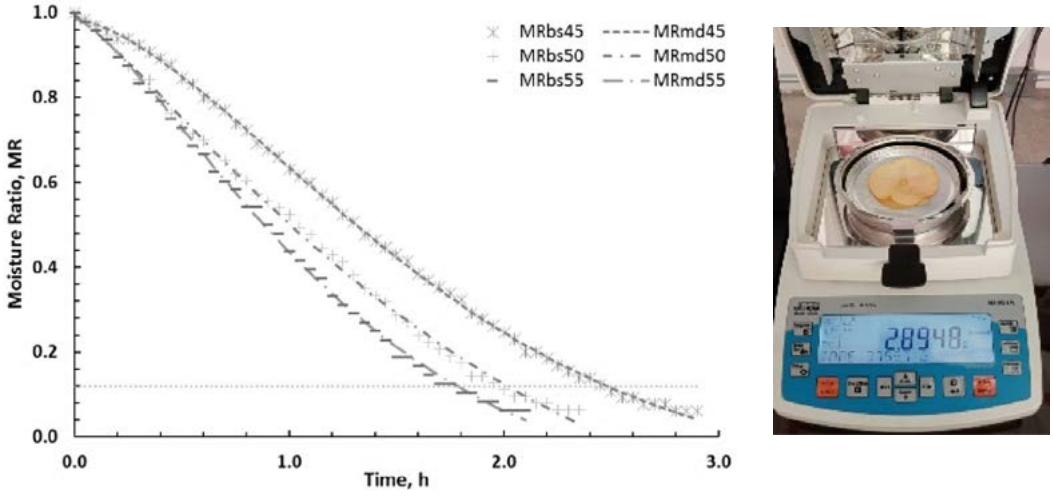

Figure 5. Deshydration of apple slices: (a) MR_{ex} y MR_{est}, *vs t*. (b) during the dehydration process. Source: Authors.

Plotting *t vs.* T yielded the expression to define the time at which *MR* is reduced to 10±2% with R^2=0.95, Equation 19:

$$t = -0.08T + 6.45 \quad (19)$$

According to Nadi and Tzempelikos (2018), the values of *t* for a similar T ranged between (5-4) h, which was lower by (50-60) % compared to the results obtained here, demonstrating that T was the main factor influencing the duration of dehydration.

Dehydration Rate

The primary factor influencing the dehydration of apple slices was temperature; that is, at higher T, the values of D_{eff} and vapor pressure deficit increased (Dufera *et al.*, 2021). The values of DR ranged between (0.005-0.016) $kg_{H_2O}\ kg_{MS^{-1}}\ min^{-1}$ for T=(45-55) °C, similar to (0.001-0.05) $kg_{H_2O}\ kg_{MS^{-1}}\ min^{-1}$ obtained by Nadi and Tzempelikos (2018). These values were consistent for all temperatures, where stability in DR was more evident. Plotting DR *vs.* T generated Equation 20 with R^2=0.97.

$$DR = 0.0813 \cdot e^{(0.0312 \cdot T)} \quad (20)$$

As T increased, the values of DR also increased due to the increase in water vapor concentration on the saturated surface of the slices; however, higher T values could cause greater shrinkage and product deterioration.

Mathematical modeling

Table 2 presents the mathematical modeling for dehydrating apple slices at different temperatures, where the Midilli-K model showed the best fit of the curves MR_{ex} *vs.* MR_{est}, with R^2=0.9987, RMSE=0.0108 and SSE=0.0054, followed by the Logarithmic and Kaleta models with R^2=(0.9963 and 0.9957). This is consistent with Noori *et al.* (2021) where this model showed a better fit to the data.

Adjustment in the Constant and Coefficients of the Model

The effect of temperature (T) on the dehydration constant, *k*, and the coefficients of the Midilli-K model was studied, along with their adjustment and validation.

The statistics for these parameters ranged from (0.9980-0.9994) for R^2, from 0.0076-0.0138 for RMSE, and (0.0032-0.0084) for SSE (Table 2). To fit the model to the data, Equation 21 expressed *MR* as a function of *k*, *a*, *n*, and *b*.

$$MR(k,a,n,b) = \frac{MR}{MR_0} = ae^{(-kt^n)} + bt \quad (21)$$

The values of *k* were directly proportional to T and were modified based on the properties of the product. From the graph of *k vs.* T, Figure 6, Equation 22 was obtained with an R^2=0.99

Table 2. Coefficients and statistics of the dehydration models, where: i) Kaleta, ii) Two-T., iii) Henderson and P., iv) Logarithmic, v) Midilli-K., vi) Page, vii) Diffusion Approximation and viii) Verma.

Model	T (°C)	Coeffs,	Values				R^2	RMSE	SSE
i	45	*k*,*a*	8.46	0.36	0.37	1.32	0.998	0.0105	0.0138
	50		−15.32	0.68	0.68	1.44	0.994	0.0240	0.0234
	55		3.30	0.86	0.86	1.49	0.996	0.0136	0.0187
ii	45	k_0,*a* k_1,*b*	−13.32	0.68	14.47	0.68	0.957	0.2343	0.0653
	50		11.10	0.23	−10.07	0.19	0.997	0.0990	0.0454
	55		4.62	0.29	−3.58	0.17	0.969	0.1200	0.0555
iii	45	*k*,*a*	1.14	0.71			0.955	0.2485	0.0660
	50		1.10	0.89			0.966	0.1400	0.0552
	55		1.12	1.02			0.967	0.1255	0.0553
iv	45	*k*,*a* *c*	2.33	0.20	−1.28		0.994	0.0286	0.0226
	50		1.89	0.32	−0.87		0.997	0.0106	0.0154
	55		1.75	0.42	−0.71		0.996	0.0131	0.0181
v	45	*k*,*a* *n*,*b*	0.98	0.40	1.60	−0.02	0.999	0.0032	0.0076
	50		0.99	0.54	1.24	−0.08	0.998	0.084	0.0138
	55		0.99	0.73	1.39	−0.04	0.998	0.0046	0.0109
vi	45	*k*,*n*	0.46	1.65			0.997	0.0129	0.0150
	50		0.72	1.46			0.992	0.0296	0.0254
	55		0.86	1.49			0.996	0.0136	0.0182
vii	45	*k*,*n*	8.74	0.09	0.54		0.958	0.2313	0.0643
	50		11.05	0.17	0.77		0.996	0.0410	0.0302
	55		0.69	0.90	1.00		0.949	0.1983	0.0704
viii	45	*k*,*a* *g*	−10.86	0.05	0.08		0.993	0.0383	0.0261
	50		−37.78	0.28	0.28		0.996	0.0130	0.0170
	55		175.20	1.36	1.36		0.969	0.1172	0.0541

Source: Authors.

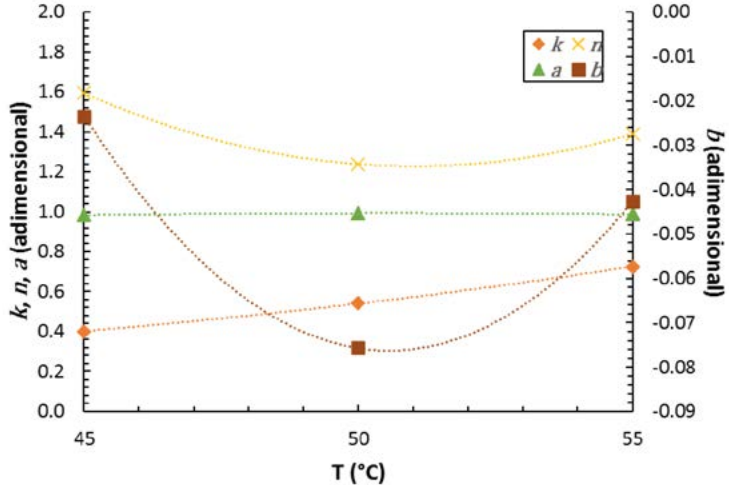

Figure 6. Midilli model constant, *k*, and *a*, *n*, *b*, *vs.* T. Source: Authors.

$$k = 0.0283 \cdot e^{(0.0590 \cdot T)} \quad (22)$$

The values of *a* and *n* maintained a positive relationship with respect to T. The graph of *a vs.* T showed a dispersion of R^2=0.925, with an average of *a*=0.9888. Plotting *n vs.* T resulted in a dispersion of R^2=0.9909, with *n*=1.408. Meanwhile, *b* maintained a negative relationship with T. Through the *b vs.* T curve with R^2=0.9925, an average of *b*=−0.0472 was obtained. It is worth mentioning that for fitting the model, it was not necessary for all parameters to show a similar dispersion among them.

Generalization of the MR Curve

The possibility of adjusting a general expression to the apple slice dehydration data based on the Midilli-K model was verified to determine the *MR* values *vs.* τ for each T. For this purpose, the value of *k* from Equation 22 and the average of the parameters *a*, *n*, and *b* were substituted into Equation 21. Thus, the general expression to model the process was derived as Equation 23.

$$MR_{aj} = 0.99e^{\left[-(k)\tau^{1.41}\right]} - 0.0473\tau \quad (23)$$

Model Validation

MR_{aj} *vs.* MR_{ex} was contrasted, showing an average dispersion of R^2=0.99 around the fit line (Table 3), thus demonstrating the effectiveness of the adjusted model for dehydrating apple slices.

Effective Diffusivity and Activation Energy

Effective Diffusivity

To correlate ln(*MR*) *vs. t*, linear regression was applied, with an average goodness of fit of R^2=0.98, Equation 24 (Table 3).

$$\ln(MR) = At + B \quad (24)$$

where *A* and *B* (dimensionless) are temperature-dependent constants.

D_{eff} was obtained according to k_o and *L*, Equation 7. Increasing T led to increased D_{eff} values ranging between, (89.83 E^{-08}-1.24 E^{-06}) $m^2\ s^{-1}$, with R^2=0.96 (Table 4). These

Table 3. Correlation of MR_{ex} *vs.* MR_{aj} and coefficients of ln(*MR*), with k_o *t*, for different temperature values.

T (°C)	MR_{aj} - MR_{aj}	R^2	Coeficientes		R^2
			A=−k_o	B	
45	0.98·MR−0.01	0.99	−0.99	0.39	0.94
50	1.00·MR+0.02	0.99	−1.20	0.34	0.95
55	1.02·MR−0.01	0.99	−1.36	0.33	0.96

Source: Authors.

values fall within the permissible range for dehydrating food products, (10^{-11}-10^{-6}) $m^2\ s^{-1}$ (Olanipekun *et al*, 2015). This differs from Beigi (2016), who reported D_{eff} values of (6.75 E^{-10}-1.28 E^{-09}) $m^2\ s^{-1}$, in a range of T=(50-70) °C, with v=(1-2) m s^{-1}.

When contrasting D_{eff} *vs. MR* at different temperatures, D_{eff} values were directly proportional to T. The maximum values were obtained when MR_{ex} decreased, *i.e.*, at the end of dehydration. This allowed verifying that, at higher T, D_{eff} values increased, resulting in a shorter duration of the process. In other words, the internal mass transfer of the product was achieved by diffusion rather than evaporation on the surface. Consequently, the moisture content was extracted in a shorter period of time.

Activation Energy

With the slope and intercept of the $\ln(D_{eff})$ *vs.* 1 T^{-1} line, Equation 25, R^2=0.98, the values of the pre-exponential Arrhenius factor, D_o, and activation energy, E_a, in apple slices were 3.74 E^{-02} $m^2\ s^{-1}$ y 28.11 kJ mol^{-1}, similar to the 23.42 kJ mol^{-1} reported by (Martynenko and Janaszek, 2014), where E_a falls within the permissible range for processing foods and agricultural products.

$$\ln\left(D_{eff}\right) = -\frac{3380.46}{T} - 3.29 \tag{25}$$

The above result was 2.8 kJ mol^{-1} lower than the E_a obtained by Meisami-asl *et al.* (2010) in the Golab variety, meaning in this case, the energy requirements and process costs for dehydrating the product should be 9% lower.

Thermodynamic Properties

During the dehydration of apple slices, the influence of enthalpy, entropy, and Gibbs free energy was observed (Table 4), obtaining positive values of ΔH, which, as T increased, decreased from 25.46-25.38 kJ mol^{-1}, meaning that higher T requires less energy to remove moisture content from the product (Oliveira *et al.*, 2010).

Meanwhile, the values of ΔS decreased from −0.2728-−0.2730 kJ mol^{-1} K^{-1}; these negative values indicate chemical adsorption or structural modifications in the product (Almeida *et al.*, 2021), *i.e.*, on its surface due to water vapor.

Finally, ΔG increased from (112.25-114.98) kJ mol^{-1}, as observed by Nadi and Tzempelikos (2018) when dehydrating apple slices, who obtained ΔG=(118.27-123.39) kJ

Table 4. D_{eff} and Thermodynamic Properties in the Dehydration of Apple Slices.

T (°C)	D_{eff} ($m^2\ s^{-1}$)	ΔH (kJ mol^{-1})	ΔS (kJ mol^{-1} K^{-1})	ΔG (kJ mol^{-1})
45	89.83 E^{-08}	25.46	−0.2727	112.25
50	01.09 E^{-06}	25.42	−0.2729	113.61
55	01.24 E^{-06}	25.38	−0.2730	114.98

Source: Authors.

mol^{-1} for T=(50-70) °C. The positive values indicate that external energy input is required for the process to occur, as it does not happen spontaneously (Nadi and Tzempelikos, 2018). Accordingly, for the studied range of T, the values of ΔH, ΔS, and ΔG can be determined using Equations (26-28), with

R^2 values of 0.9999, 0.9997 y 0.9998.

$$\Delta H = -8.31T + 25835.40 \quad (26)$$

$$\Delta S = -0.0257T - 271.63 \quad (27)$$

$$\Delta G = 272.92T + 99967.81 \quad (28)$$

Total Phenolic Compounds and Antioxidant Activity

Total Phenolic Content

This parameter, determined in the dehydrated apple samples, can be observed in Figure 7, where the initial total phenolic content was 168.67±2.16 mg EAG 100 g^{-1} of the fresh sample. Among the evaluated dehydration temperatures, the treatment at 45 °C presented the highest amount of phenolic compounds with 51.1±1.54 mg EAG 100 g^{-1}. For the dehydration treatments of the apple slices at 50 and 55 °C, the analysis of variance showed that there was no statistically significant difference ($p \leq 0.05$). It was observed that the increase in dehydration temperature caused a degradation of the total phenols with respect to the content present in the sample.

Several studies have demonstrated that different factors such as variety, geographical region of cultivation, and even the botanical fraction used for determination (skin, pulp, and whole fruit) have an effect on the total phenolic content (CFT) (Biedrzycka *et al.*, 2008). In a study by Corona-Leo *et al.* (2020), seven apple varieties were evaluated, showing a statistically significant difference ($p \leq 0.05$) in CFT present in the skin, pulp,

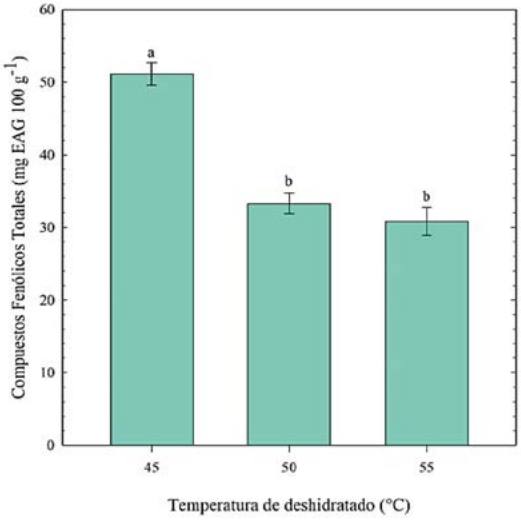

Figure 7. Total phenolic content in dehydrated Golden Delicious apple slices at three different temperatures. The columns represent the mean of $n=3$ replicates ± standard error.

and whole fruit. The authors also reported that the highest CFT was found in the skin of all apple varieties, ranging from 109.20-257.20 mg EAG 100 g^{-1} in the Golden Delicious imported and Granny Smith varieties, respectively. Regarding the whole fruit, TPC values ranged from 137.2 mg EAG 100 g^{-1} in Golden Delicious to 315.87 mg EAG 100 g^{-1} in Granny Smith apples. These values are consistent with the results obtained in this research (168.67±2.16 mg EAG 100 g^{-1}) for fresh apple samples. In another study by Rana *et al.* (2021), the CFT determined by the Folin-Ciocalteu assay varied between 219±0.09 and 459±0.47 mg EAG 100 g^{-1} in a comparative evaluation of five apple varieties grown in the Western Himalayas, including the Golden Delicious variety, whose value is higher than that reported in this work. Pires *et al.* (2018) quantified the CFT in the 'Bravo de Esmolfe' variety using high-performance liquid chromatography with a diode array detector coupled to mass spectrometry (HPLC-DAD-ESI-MS), obtaining 237±1 mg EAG 100 g^{-1} for the hydro-methanolic extracts of their samples, confirming that CFT in fresh apple fruits is strongly associated with fruit variety.

Furthermore, various studies have shown that multiple factors affect CFT due to the dehydration process; however, the most significant effect corresponds to temperature. In this regard, efforts have been made to determine the optimal conditions to ensure product quality, particularly in minimizing changes in bioactive compounds such as phenolic compounds. In the study by Kahraman *et al.* (2021), three methods were evaluated to characterize dehydration and quality attributes in slices of *Malus×domestica* Borkh var. Gala apples, where the authors reported the highest CFT by the freeze-drying method (68.82 mg EAG 100 g^{-1}) and the lowest value (16.12 mg EAG 100 g^{-1}) by the hot air dehydration method at 60±1 °C. These values were approximately consistent with the experimental results obtained in the present study; however, it should be noted that the evaluated fruit variety was different.

CFT is associated with the antioxidant capacity of biological products; however, it is known that phenols are sensitive to temperature. Therefore, the main focus of this study was to find process conditions that would allow the product to be dehydrated while retaining the highest amount of bioactive compounds, as phenolic compounds are functional food nutrients with excellent antioxidant and anti-inflammatory capabilities (Wang *et al.*, 2023).

Antioxidant Activity

DPPH and ABTS Radical Scavenging Assays

The initial radical scavenging activity in the fresh sample was 766.9±91.4 and 973.3±103.4 μg mg^{-1} according to the DPPH and ABTS methods, respectively (Figure 8), where it was confirmed that the highest values of antioxidant activity showed an inverse behavior with respect to the dehydration temperature; that is, the highest antioxidant activity was observed at the lowest dehydration temperature (45 °C). In this regard, Demiray *et al.* (2023) evaluated the effect of three temperatures (45, 55, and 65 °C) on two thicknesses of Granny Smith apple slices (1.5 and 5 mm), where the highest antioxidant capacity values were observed, unlike this study, at 55 °C with 34.44 and 31.45 μmoles equivalents of Trolox for 1.5 and 5 mm thicknesses.

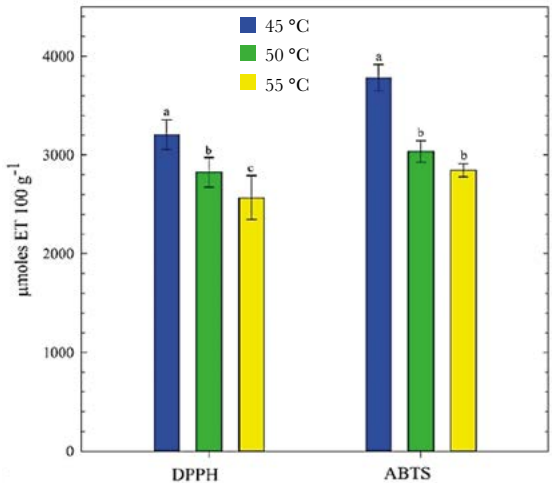

Figure 8. Effect of dehydration temperature and the method of antioxidant activity evaluation using DPPH and ABTS assays, where each column represents the mean of $n=3$ replicates ± standard error.

Additionally, the results showed that the ABTS assay produced higher values of antioxidant activity compared to those determined by DPPH for all three temperatures. In this regard, it has been mentioned that most methods are limited by the antioxidant extraction technique, as some compounds may remain forming complexes in the extraction residues (Serrano *et al.*, 2007).

On the other hand, the differences between the antioxidant capacity of the fresh sample and that after the dehydration process could be attributed to the generation of Maillard reaction-derived compounds by pyrolysis, which can enhance antioxidant capacity and FRAP during dehydration at moderately high temperatures (López-Vidaña *et al.*, 2019). Antioxidant compounds could be promising agents for managing diseases related to oxidative stress. The results demonstrated that, for the case study, the temperature of 45 °C could prevent the destruction of total phenolics and compounds with antioxidant activity in dehydrated apple slices.

CONCLUSIONS

The kinetics of thin-layer dehydration of apple slices was studied through mathematical modeling to evaluate the effect of temperature on the moisture ratio of the product. As the temperature increased, the processing time for the product between 45 and 55 °C decreased from 174-126 minutes. It was demonstrated that the Midilli-K. model better described the dehydration process, showing the best goodness of fit to the data. The effects of temperature on the constant and coefficients of the model were studied, with this constant being directly proportional to temperature. The dehydration rate, effective diffusivity, and activation energy in apple slices increased with increasing temperature. The thermodynamic properties of the process were determined under the established dehydration conditions. As the temperature increased, the enthalpy and entropy decreased, with the latter values being negative, while the Gibbs free energy increased. With the information obtained, it could be possible to establish the temperature and time at which

Symbols and Abbreviations.

Symbol	Description
AER	Radical scavenging activity (%)
A, *B*	Temperature-dependent constants, dimensionless
ABTS	2,2'-Azinobis-(3-ethylbenzothiazoline-6-sulfonic acid)
aj	Adjusted
A_o	Absorbance of blank or control sample
A_s	A of sample extract
A_{t_0} , A_{t_6}	A during time intervals t=0.6
a, *e*, *n*, *b*, *c*, *g*	Time-dependent constants, dimensionless
DR	Dehydration rate $\left(kg_{H_2O}\ kg_{MS^{-1}}\ min^{-1}\right)$
D_o	Frequency or pre-exponential factor of Arrhenius ($m^2\ s^{-1}$)
D_{eff}	Effective diffusivity ($m^2\ s^{-1}$)
DHS	Significant honest difference
DPPH	2.2-diphenyl-1-picrylhydrazyl
Δ	Increment
EAG	Gallic acid equivalents
E_a	Activation energy ($J\ mol^{-1}$)
est	Estimated
ex	Experimental
F_o	Fourier number (dimensionless)
G	Gibbs free energy ($J\ mol^{-1}$)
H	Enthalpy ($J\ mol^{-1}$)
h_P	Planck's constant ($6.626{\cdot}E^{-34}\ J\ s^{-1}$)
inh	Inhibition
k_B	Boltzmann constant ($1.38{\cdot}E^{-23}\ J\ K^{-1}$)
k_o	Slope of ln(*MR*) *vs. t* line
L	Material thickness (m)
MR	Moisture ratio (dimensionless)
M_t	Moisture ratio at time t $\left(g_{H_2O}\ g_{MS^{-1}}\right)$
M_o	Initial moisture ratio of product $\left(g_{H_2O}\ g_{MS^{-1}}\right)$
M_e	Equilibrium moisture ratio $\left(g_{H_2O}\ g_{MS^{-1}}\right)$
MR_o	*MR* initial (dimensionless)
m	Mass, kg
N_c	Dehydration rate constant ($1\ min^{-1}$)
n	Number of terms (dimensionless)
R	Universal gas constant ($8.3143\ J\ mol^{-1}\ K^{-1}$)
R^2	Coefficient of determination
RMSE	Root mean square error
SSE	Sum of squares due to error
S	Entropy ($J\ mol^{-1}\ K^{-1}$)
T	Absolute temperature (K)
T	Temperature, °C
t	Time, min
τ	Time (dimensionless)
v	Air velocity, ms^{-1}

apple slices could be processed according to local climatology, whether dehydrating the product outdoors or under controlled systems.

ACKNOWLEDGEMENTS

The authors thank the Universidad Anáhuac Veracruz and Instituto Tecnológico Superior de Xalapa for funding this research.

AUTHORS' CONTRIBUTIONS

For this work, the authors performed the following activities:

Conceptualization: Laureano-López, B.; Daza-Merino, C. A.; Santos-Hernández, A. M. Data acquisition: Laureano-López, B.; Santos-Hernández, A. M.; Riviello-Flores, M. L. Data analysis: Laureano-López, B.; Daza-Merino, C. A.; Santos-Hernández, A. M.; Daza-Merino, R.

Methodology design: Laureano-López, B.; Daza-Merino, C. A.; Santos-Hernández, A. M.

Writing and editing: Laureano-López, B.; Santos-Hernández, A. M.; Riviello-Flores, M. L.; Daza-Merino, R.

CONFLICT OF INTEREST STATEMENT

The authors declare no conflict of interest.

REFERENCES

Almeida, R. L. J., Santos, N. C., Alves, I. L., and André, A. M. M. C. N. (2021). Evaluation of thermodynamic properties and antioxidant activities of Achachairu (*Garcinia humilis*) peels under drying process. *Flavour and Fragrance Journal*, 36, 213-222.

Araujo, W. D., Goneli, A. L. D., Corrêa, P. C., Hartmann, C. P., and Martins, E. A. S. (2017). Modelagem matemática da secagem dos frutos de amendoim em camada delgada1. *Revista Ciência Agronômica, 48*(3), 448-457. https://doi.org/10.5935/1806-6690.20170052

Bao, X.; Min, R.; Zhou, K.; Traffano-Schiffo, M. V.; Dong, Q. and Luo, W. (2023). Effects of vacuum drying assisted with condensation on drying characteristics and quality of apple slices. *Journal of Food Engineering*, 340: 111286. https://doi.org/10.1016/j.jfoodeng.2022.111286

Beigi, M. (2016). Energy efficiency and moisture diffusivity of apple slices during convective drying. *Food Science and Technology*, 36, 145-150.

Benseddik, A., Azzi, A., Zidoune, M. N., and Allaf, K. (2018). Mathematical empirical models of thin-layer airflow drying kinetics of pumpkin slice. *Engineering in Agriculture, Environment and Food*, 11, 220-231.

Beye, N. F., Kane, C., Ayessou, N., Kebe, C. M. F., Talla, C., Diop, C. M., and Sène, A. (2019). Modelling the dehydration kinetics of four onion varieties in an oven and a solar greenhouse. *Heliyon*, 5. https://doi.org/10.1016/j.heliyon.2019.e02430

Celma, A. R., Rojas, S., López, F., Montero, I., and Miranda, T. (2007). Thin-layer drying behaviour of sludge of olive oil extraction. *Journal of Food Engineering*, 80, 1261-1271.

Corona-Leo, L. S.; Hernández-Martínez, D. M. and Meza-Márquez, O. G. (2020). Analysis of physicochemical parameters, phenolic compounds and antioxidant capacity of peel, pulp and whole fruit of five apple varieties (*Malus domestica*) harvested in Mexico. *Biotecnia, 22*(1): 166-174.

Corona-Leo, L. S.; Meza-Márquez, O. G. and Hernández-Martínez, D. M. (2021). Effect of *in vitro* digestion on phenolic compounds and antioxidant capacity of different apple (*Malus domestica*) varieties harvested in Mexico. *Food Bioscience*, 43: 101311. https://doi.org/10.1016/j.fbio.2021.101311

Costa, C. F., Corrêa, P. C., Vanegas, J. D. B., Baptestini, F. M., Campos, R. C., and Fernandes, L. S. (2016). Mathematical modeling and determination of thermodynamic properties of jabuticaba peel during the drying process. *Revista Brasileira de Engenharia Agrícola e Ambiental*, 20, 576-580.

Crank, J. (1979). The mathematics of diffusion. Oxford university press.

Demiray, E.; Gamze, Y., J.; Aktok, Ö.; Çulluk, B.; Çalıskan, K., G. and Pandiselvan, R. (2023). The Effect of Drying Temperature and Thickness on the Drying Kinetic, Antioxidant Activity, Phenolic Compounds, and Color Values of Apple Slices. *Journal of Food Quality*, vol. 2023, Article ID 7426793, 12 pp. https://doi.org/10.1155/2023/7426793

Dufera, L. T., Hofacker, W., Esper, A., and Hensel, O. (2021). Experimental evaluation of drying kinetics of tomato (*Lycopersicum esculentum* L.) slices in twin layer solar tunnel dryer. *Energy for Sustainable Development*, 61, 241-250.

Ekka, J. P., and Palanisamy, M. (2020). Determination of heat transfer coefficients and drying kinetics of red chilli dried in a forced convection mixed mode solar dryer. *Thermal Science and Engineering Progress*, 19, 100607.

FAOSTAT. (2023). Cultivos y productos de ganadería. Retrieved July 10, 2023, from United Nations Organization para la Alimentación y la Agricultura taken from: https://www.fao.org/faostat/es/#data/QCL

Frei, B. 1994. Natural antioxidants in human health and disease. United Kingdom: Academic Press. 592 p.

Ghasemkhani, H., Khoshnam, F., and Kamandar, M. R. (2021). Drying Apple Slices in a Rotating-Tray Convective Dryer: A Study on Dehydration Characteristics and Qualitative Attributes. *Iranian Journal of Chemical Engineering (IJChE)*, 18, 16-32.

Ghinea, C., Prisacaru, A. E., and Leahu, A. (2022). Physico-Chemical and Sensory Quality of Oven-Dried and Dehydrator-Dried Apples of the Starkrimson, Golden Delicious and Florina Cultivars. *Applied Sciences*, 12, 2350.

Inyang, U. E., Oboh, I. O., and Etuk, B. R. (2018). Kinetic Models for Drying Techniques—Food Materials. *Advances in Chemical Engineering and Science*, 8, 27-48.

Iordănescu, O. A.; Bala, M.; Iuga, A. C.; Gligor, D.; Dascălu, I.; Bujancă, G. S.; David, I.; Hădărugă, N. G. and Hădărugă, D. I. (2021). Antioxidant Activity and Discrimination of Organic Apples (*Malus domestica* Borkh.) Cultivated in the Western Region of Romania: A DPPH Kinetics–PCA Approach. *Plants*, 10: 1957. https://doi.org/10.3390/plants10091957

Jideani, V. A., and Mpotokwana, S. M. (2009). Modeling of water absorption of Botswana bambara varieties using Peleg's equation. *Journal of Food Engineering, 92*(2), 182-188. https://doi.org/10.1016/j.jfoodeng.2008.10.040

Kahraman, O.; Malvandi, A.; Vargas, L. and Feng, H. (2021). Drying characteristics and quality attributes of apple slices dried by a non-thermal ultrasonic contact drying method. *Ultrasonics Sonochemistry*, 73, 105510. https://doi.org/10.1016/j.ultsonch.2021.105510

Kaleta, A., Górnicki, K., Winiczenko, R., and Chojnacka, A. (2013). Evaluation of drying models of apple (var. Ligol) dried in a fluidized bed dryer. *Energy Conversion and Management*, 67, 179-185.

López-Vidaña, E. C.; Pilatowsky F. I.; Antonio, M. E. G.; Navarro-Ocaña, A.; Hernández-Vázquez, L. and Santiago-Urbina, J. A. (2019). Solar drying kinetics and bioactive compounds of blackberry (*Rubus fruticosus*). *Journal of Food Process Engineering, 42*(4): e13018. https://doi.org/10.1111/jfpe.13018

Martynenko, A., and Janaszek, M. A. (2014). Texture Changes During Drying of Apple Slices. *Drying Technology*, 32, 567-577.

Meisami-asl, E., Rafiee, S., Keyhani, A., and Tabatabaeefar, A. (2010). Drying of apple slices (var. Golab) and effect on moisture diffusivity and activation energy. Plant Omics. Recuperado de https://www.semanticscholar.org/paper/Drying-of-apple-slices-(var.-Golab)-and-effect-on-Meisami-asl-Rafiee/09cca6b9cb9fecf726507e9383127e5dca1976fe

Menezes, M. L. de, Kunz, C. C., Perine, P., Pereira, N. C., Santos, O. A. A. dos, and Barros, S. T. D. de. (2013). Analysis of convective drying kinetics of yellow passion fruit bagasse. *Acta Scientiarum. Technology*, 35. https://doi.org/10.4025/ACTASCITECHNOL.V35I2.10286)

Mghazli, S., Ouhammou, M., Hidar, N., Lahnine, L., Idlimam, A., and Mahrouz, M. (2017). Drying characteristics and kinetics solar drying of Moroccan rosemary leaves. *Renewable Energy*, 108, 303-310.

Mohammadi, I., Tabatabaekoloor, R., and Motevali, A. (2019). Effect of air recirculation and heat pump on mass transfer and energy parameters in drying of kiwifruit slices. *Energy*, 170, 149-158.

Mugodo, K., and Workneh, T. S. (2021). The kinetics of thin-layer drying and modelling for mango slices and the influence of differing hot-air drying methods on quality. *Heliyon*, 7, e07182.

Nadi, F., and Tzempelikos, D. (2018). Vacuum drying of apples (cv. Golden Delicious): Drying characteristics, thermodynamic properties, and mass transfer parameters. *Heat and Mass Transfer*, 54, 1853-1866.

Noori, A. W., Royen, M. J., and Haydary, J. (2021). Thin-layer mathematical modeling of apple slices drying, using open sun and cabinet solar drying methods. *International Journal of Innovative Research and Scientific Studies*, 4, 43-52.

Olanipekun, B. F., Tunde-Akintunde, T. Y., Oyelade, O. J., Adebisi, M. G., and Adenaya, T. A. (2015). Mathematical Modeling of Thin-Layer Pineapple Drying. *Journal of Food Processing and Preservation*, 39, 1431-1441.

Olawoye, B. T., Kadiri, O., and Babalola, T. R. (2017). Modelling of thin-layer drying characteristic of unripe Cardaba banana (*Musa* ABB) slices. *Cogent Food and Agriculture, 3*(1), 1290013.

Oliveira, G. H. H. de, Corrêa, P. C., Araujo, E. F., Valente, D. S. M., and Botelho, F. M. (2010). Desorption isotherms and thermodynamic properties of sweet corn cultivars (*Zea mays* L.). *International Journal of Food Science and Technology*, 45, 546-554.

Petković, M., Lukyanov, A., Rudoy, D., Kurćubić, V., Đurović, I., Miletić, N., and Safarov, J. (2021). Potato thin layer convective dehydration model and energy efficiency estimation. E3S Web of Conferences, 273, 07028.

Pires, T. C. S. P.; Dias, M. I.; Barros, L.; Alves, M. J.; Oliveira, M. B. P. P.; Santos-Buelga, C. and Ferreire, I. C. F. R. (2018). Antioxidant and antimicrobial properties of dried Portuguese apple variety (*Malus domestica* Borkh. cv Bravo de Esmolfe). *Food Chemistry*, 240: 701-706. http://dx.doi.org/10.1016/j.foodchem.2017.08.010

Rana, S.; Rana, A.; Gupta, S. and Bushman, S. (2021). Varietal influence on phenolic constituents and nutritive characteristics of pomace obtained from apples grown in western Himalayas. *Journal of Food Science and Technology, 58*(1): 166-174. https://doi.org/10.1007/s13197-020-04526-y

Royen, M. J., Noori, A. W., and Haydary, J. (2020). Experimental Study and Mathematical Modeling of Convective Thin-Layer Drying of Apple Slices. *Processes*, 8, 1562.

Sabarez, H. T. (2015). Commonwealth Scientific and Industrial Research Organisation–Food and Nutrition Flagship, Werribee, Victoria, Australia. *Modeling Food Processing Operations*, 95.

Serrano, J.; Goñi, I.; Saura-Calixto, F. (2007). Food antioxidant capacity determined by chemical methods may underestimate the physiological antioxidant capacity. *Food Research International*, 40: 15-21. https://doi.org/10.1016/j.foodres.2006.07.010

Şĭmşek, M., Küçük, H., and Mĭdĭllĭ , A. (2021). Experimental Investigation and Mathematical Modeling of Microwave Thin Layer Drying Behaviour of Apricot, Kiwi and Mint Leaves. *Recep Tayyip Erdoğan Üniversitesi Fen ve Mühendislik Bilimleri Dergisi*, 2, 13-35.

Solano, E. M. V., and Rodríguez, F. A. G. (2010). Designing, assembly and start up for a semiautomatic hot-air tray dryer. *Ingeniería e Investigación*, 30, 43-51.

Tunckal, C., Coskun, S., Doymaz, İ., and Ergun, E. (2018). Determination of sliced pineapple drying characteristics in a closed loop heat pump assisted drying system. *International Journal of Renewable Energy Development-IJRED, 7*(1).

Tunçkal, C. (2020). Investigation of performance and drying kinetics of the closed, partially open, and open heat pump drying systems. *Journal of Food Process Engineering*, 43, e13566.

Wang, H.; Zhang, Z.; Song, J. Tian, M., Li, R. and Cui, X. (2023). Phenolic compound identification in tomato fruit by UPLC-QTOF-MS. *LWT – Food Science and Technology*, 182, 114791. https://doi.org/10.1016/j.lwt.2023.114791.